Drug Mimic Induced Conformational Changes in Model Polymer−Drug Conjugates Characterized by Small-Angle Neutron Scattering

A. Paul,*,† C. James,† R. K. Heenan,‡ and R. Schweins§

School of Chemistry, Cardiff University, Main Building, Park Place, Cardiff, CF10 3AT, United Kingdom, ISIS Facility, STFC, Rutherford Appleton Laboratories, Chilton, Didcot, Oxfordshire, OX11 0QX, United Kingdom, and Institute Laue-Langevin, BP 156, 6, rue Jules Horowitz, 38042 Grenoble Cedex 9, France

Received March 26, 2010; Revised Manuscript Received June 11, 2010

Copolymers based on poly(*N*-(2-hydroxypropylmethacrylamide)) with conjugated Doxrubicin are established as candidate anticancer therapeutics. Two HPMA-*co*-polymers (ca. 35000 g mol^{-1}) with 2.5 and 8 mol % gly-phe-leu-gly peptidyl side-chain content have been modified using linear hydrocarbon and small aromatic molecules as simple drug mimics. This first contrast-variation SANS study on these systems demonstrates, combined with detailed modeling, a controlled switch from random coil to a more defined morphology induced by inclusion of a series of model drug mimics. Relatively small changes in drug-mimic type and loading can significantly alter the solution conformation, and we tentatively propose a helical type structure that is more or less tightly wound, depending on both hydrophobe loading and type. The results presented have important implications for understanding the influence of conjugate structure on solution properties, which is an important factor influencing biological and clinical activity.

Introduction

Conjugation of drugs to water-soluble, biocompatible synthetic polymers produces polymer−drug conjugates, which have demonstrated considerable potential for the controlled, targeted delivery of drugs, particularly as anticancer therapeutics.[1−8] A variety of synthetic polymers have been investigated,[9−13] and several poly(*N*-(2-hydroxypropylmethacrylamide)) (HPMA)−drug conjugates have progressed to clinical trials as anticancer therapeutics.[2,14] Accordingly, HPMA-based conjugates are the main systems of interest in this work.

Short, enzyme-cleavable peptide sequences are frequently used to link drug molecules to the HPMA backbone; a typical conjugate structure can be found in Figure 1, along with the specific conjugates studied in this work. To match the specificity of lysosome enzyme binding sites, oligopeptide linkers need to be hydrophobic,[7,15] giving the conjugate amphiphilic properties that can, in turn, influence the drug release properties.[16] Inter- and intramolecular aggregation have also been proposed for HPMA-based conjugates, with different substituents affecting the observed behavior.[17] Understanding the interplay between solution conformation and drug delivery is, therefore, of considerable importance, and there is growing recognition that a better understanding of physicochemical properties of these systems is needed[14] Others have used both size-exclusion chromatography(SEC)/multiangle light scattering (MALS) and FRET to study HPMA-based conjugates, indicating that the addition of a drug can induce significant conformational changes.[18,19] Similarly, Ulbrich et al. demonstrated that the aggregation of hydrophobic moieties within an HPMA-based conjugate led to hindered drug release.[16]

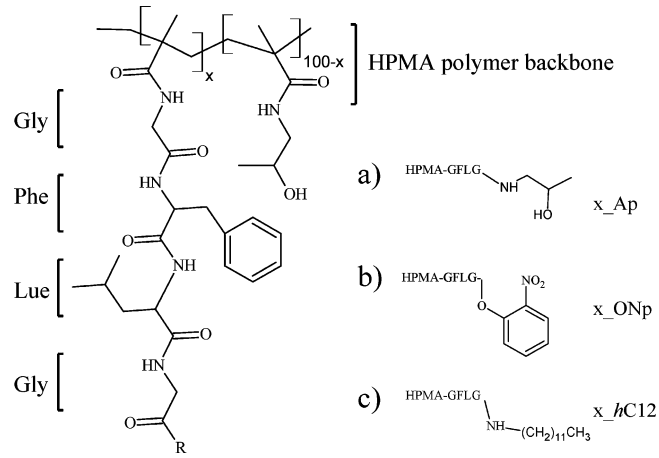

Figure 1. Structure of the HPMA-*co*-MA-GFLG copolymer where x defines the mole percent of GFLG-R side chain loading and R is the bound drug mimic: (a) aminopropanol, x_Ap; (b) *ortho*-nitrophenol, x_ONp, and (c) dodecylamine, x_*h*C12. Conjugates are therefore referred to as 5_Ap, 10_Ap, 5_ONp, 10_ONp, 5_*h*C12, and 10_*h*C12 or 10_*d*C12 in the text.

Recently, we have used small-angle neutron scattering (SANS) to better understand the global and local structure of polymer−drug conjugates in solution. In our previous work it was shown that, for a range of HPMA copolymer conjugates, both drug type and drug loading have an influence on solution conformation,[20,21] and this provided insight into overall drug release and release kinetics observed for HMPA-GFLG-doxorubicin/aminoglutethimide conjugates in development as combination therapy for hormone dependent breast cancer,[21] and ultimately for the clinically relevant HPMA−doxorubicin[20] conjugates PK1 (FCE28068) and PK2 (FCE28069) developed by Duncan et al., correlating solution conformation data with the maximum tolerated dose observed at clinical trial.[22,23]

With SANS, characterization can be carried out under physiologically relevant conditions (body temperature, biological

* To whom correspondence should be addressed. Phone: +44-(0)29 20870419. Fax: +44-(0)29 20874030. E-mail: paula3@cardiff.ac.uk.
† Cardiff University.
‡ Rutherford Appleton Laboratories.
§ Institute Laue-Langevin.

10.1021/bm1003338
Published on Web 07/01/2010

pH, ionic strength, and at a range of conjugate concentrations up to 50 mg mL^{-1}, the same as that used clinically[20]). Critically, SANS is noninvasive, and does not rely on the use of chemical modification, for example, as in the need to introduce fluorophores[19] that could themselves affect the solution conformation. Due to the length scales accessible (1−1000 Å), a significant advantage of SANS is the possibility to obtain both overall and local structural information. This can be greatly facilitated by "highlighting" different conjugate components using selective partial deuteration of the sample, and we apply this contrast variation approach to polymer−model drug conjugates for the first time in this paper.

Materials and Methods

Materials. Poly(*N*-(2-hydroxypropylmethacrylamide)) (HPMA) copolymer precursors containing two different loadings of nitrophenol (ONp) terminated gly-phe-leu-gly (GFLG) peptidyl side chains (HPMA-*co*-MA-GFLG-ONp) were purchased from Polymer Laboratories Ltd., U.K. Molecular weights were 45000 g mol^{-1} ($M_w/M_n = 1.46$) and 39000 g mol^{-1}, ($M_w/M_n = 1.74$), respectively. The precise degree of side-chain loading was determined for each polymer by UV spectroscopy ($\varepsilon_{270\ nm} = 9500$ L/mol/cm)[24] and found to be 2.6 and 8.0 mol %, respectively. By convention, conjugates are referred to hereafter by the original feedstock ratios of 5 and 10 mol %. Dodecylamine-d_{25} (99% *d*-atom) was purchased from QMX laboratories and used as received. All other reagents were used as received from Sigma-Aldrich. Conjugate synthesis was achieved by an aminolysis reaction as used previously,[20] details of which are given in the Supporting Information. The final yields for all modification reactions were between 40 and 60% with respect to polymer starting weight. The parent polymer used is potentially susceptible to hydrolysis of the ester bond, however, the measured bound/free ratio ($\lambda_{max\ (bound)} = 260$ nm, $\lambda_{max\ (free)} = 430$ nm) did not to vary up to 24 h in solution (the longest time point measured), indicating that no significant hydrolysis occurs on the time scale of the SANS experiment. The structures of the six conjugates studied are shown in Figure 1.

Small-Angle Neutron Scattering. Most SANS measurements were performed at the ISIS spallation neutron source (Rutherford Appleton Laboratories, Oxfordshire, U.K.) using the time-of-flight diffractometer, LOQ. Contrast variation experiments were performed on the D11 instrument at the Institute Laue-Langevin, Grenoble, France. Scattering data are expressed in terms of the scattering vector, Q, which is given by $Q = 4\pi/\lambda \sin(\theta/2)$, where λ is wavelength and θ is the angle at which the neutrons are scattered. The incident neutron wavelengths were 2−10 Å on LOQ, and 8 ± 1 Å on D11, giving accessible Q-ranges of 0.008−0.3 $Å^{-1}$ on LOQ and (using two sample−detector distances on D11) 0.007−0.26 $Å^{-1}$ on D11. Sample solutions were prepared at a conjugate concentration of 0.5−2 wt % on a 1 g scale in D_2O (pH 5.5, 0.1 M phosphate buffer) and placed in 2 mm path length quartz cells, mounted in a sample changer thermostatted at 37 °C (±0.2). These conditions allowed for the study of conjugates at pH, temperature, and ionic strengths mimicking those experienced during drug release in vivo. The partially deuterated conjugate sample in H_2O was prepared in an identical pH 5.5 buffer solution but at 4 wt % concentration to overcome the low signal/noise for this sample. Raw scattering data were corrected for the scattering and transmission of the solvent and cell and placed on an absolute intensity scale according to standard procedures for each instrument. Measuring times were between 45 and 90 min per sample. Data analysis was performed using the FISH modeling suite.[25]

Results

In the absence of intermolecular interactions, the intensity of scattered radiation, $I(Q)$, from a polymer solution of volume fraction ϕ_p is given by eq 1, where $\Delta\rho$ is the difference in scattering length density, ρ, between the scattering body (of volume V_p) and the solvent, and B_{inc} is the background incoherent scattering arising chiefly from hydrogen atoms in the sample.

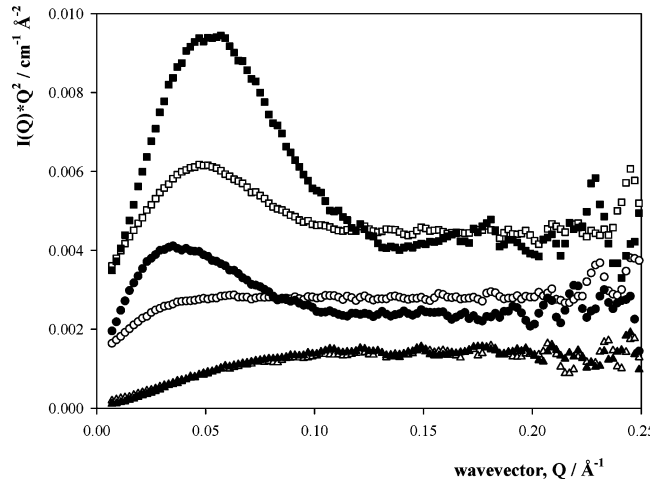

Figure 2. Kratky presentation of scattering data for conjugate solutions in D_2O/PBS at 1 wt % and 37 °C: **5_Ap** (open triangles); **10_Ap** (closed triangles); **5_ONp** (open circles); **10_ONp** (closed circles); **5_*h*C12** (open squares); and **10_*h*C12** (closed squares). For presentation purposes, ONp and *h*C12 conjugate data have been shifted by 0.0015 and 0.003 units on the *y*-axis, respectively.

$$I(Q) = \phi_p V_p (\Delta\rho)^2 P(Q,R) + B_{inc} \quad (1)$$

The form factor, $P(Q,R)$, describes the size and shape, and form factors are known for a range of particle morphologies. These can be combined with appropriate contrast and scaling terms to model the scattering data. Further details of the calculated scattering length densities and the parameters in the form factors used are given in the Supporting Information.

Figure 2 presents the raw scattering data as a Kratky representation ($I(Q)\cdot(Q^2)$ vs Q). Deviations from a Gaussian coil morphology are evident as a peak in the data, which for these molecules suggests intramolecular aggregation may be occurring. The peak positions relate to the overall size of the scattering body ($Q_{Imax} \propto 1/R_g$). This presentation therefore emphasizes differences in the raw data for the conjugates studied, and allows for a simple assessment of their likely solution morphology.[26] A comprehensive, pairwise, $I(Q)$ vs Q presentation of the data is given in the Supporting Information (Figure S2).

The Kratky plots (Figure 2) for the two aminopropanol containing conjugates are similar in shape, while plots for the two *h*-dodecyl containing conjugates are significantly different to the aminopropanol versions, but mutually similar. A change in morphology has occurred upon hydrophobic modification at 5 mol % *h*-dodecyl content (**5_*h*C12**) that is retained on increasing the loading (**10_*h*C12**). Kratky plots for the *ortho*-nitrophenol terminated systems, however, show a change in shape from 5% *ortho*-nitrophenol (**5_ONp**), where a small bump in the data is discernible at $Q \sim 0.06-0.08$, to a more pronounced maxima for 10% *ortho*-nitrophenol (**10_ONp**), ultimately giving a profile similar to that of the *h*-dodecyl-substituted conjugates.

The shape of the Kratky plots are therefore consistent with (i) Gaussian coil morphology for both aminopropanol containing conjugates, (ii) random coil for 5% *ortho*-nitrophenol **(5_ONp)**, with a change in shape observed on increasing the loading to

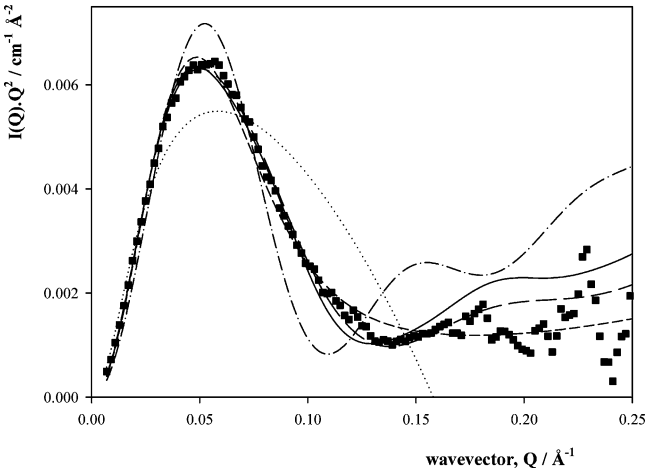

Figure 3. Scattering data for **10_*h*C12** with "best" fits to form factors for: polydisperse coils (dotted line); solid ellipse (long dashed line); monodisperse spheres (dash-dot line); polydisperse spheres (short dashed line); and rods (solid line).

10_ONp, and (iii) nonrandom coil structure for both *h*-dodecyl containing conjugates conjugates.

For the aminopropanol terminated conjugates, an upturn is present in the data at low Q values (Figure S2). This has been observed previously[20] and suggests the presence of either an attractive structure factor that is not concentration dependent across the measured range or some degree of intermolecular aggregation.

A more quantitative assessment of polymer conformation may be obtained from the radius of gyration of a polymer (R_g). This can be found from fitting the data to a model for polydisperse Debye coils, giving R_g values of 55 ± 2 for 5 mol % and 43 ± 2 Å at 10 mol % loading. Substitution of aminopropanol groups with *ortho*-nitrophenol or dodecyl groups rendered the coil model inappropriate for all but the lowest *ortho*-nitrophenol loading (**5_ONp**), for which $R_g = 74 \pm 2$ Å. Alternative models for other conjugates data were therefore sought, and after extensive analysis, a rod-like morphology was found to be the most appropriate, Figure 3. (A full validation of the modeling approach is given in the Supporting Information).

Validity of the rod model is further demonstrated when we consider the conjugate in which the alkyl chains have been deuterated (sample **10_*d*C12**). This introduces a scattering length density difference ($\Delta\rho$) between the hydrophobes and the linker/polymer backbone, allowing the various parts of the structure to be highlighted in different solvents, see Figure 4a. Aggregation of the hydrophobes would then induce a difference in scattering length density between the hydrophobic domain and the polymer backbone/linkers, which would manifest as a "bump" in $I(Q)$ versus Q plot high Q values. This feature provides a direct indication of a characteristic 'short' dimension in the structure ($Q_{max} = 2\pi/d$).

The conjugate containing deuterated dodecyl chain substituents (**10_*d*C12**) was studied as a solution in H_2O and D_2O, which in combination with the **10_*h*C12** sample in D_2O provides a full contrast set of hydrophobe/(polymer and linker)/solvent of D/H/H, D/H/D, H/H/D, to give scattering from the core only/shell only/whole conjugate, using solid rod/core−shell rod/and solid rod models, respectively (see Figure 4a).

For these conjugates the "sharpness" of these core/shell interfaces are complicated somewhat by the presence of the peptidyl linkers, which have scattering length densities intermediate between the polymer backbone (especially evident in

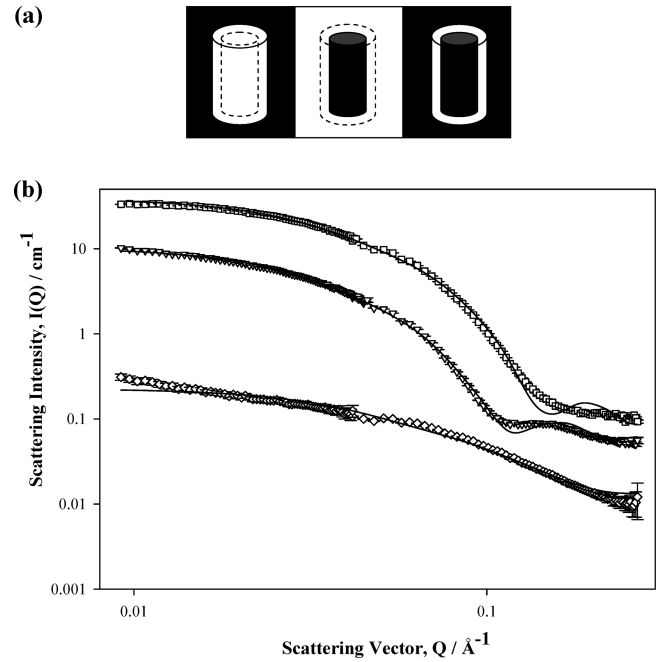

Figure 4. (a) Schematic representation of the contrast-variation scattering experiment for a core−shell rod: white denotes hydrogenous components and black denotes deuterated components. (b) Scattering data and fits obtained for the **10_*h*C12** and **10_*d*C12** contrast-variation experiment: **10_*h*C12** in D_2O/PBS (whole structure; open squares); **10_*d*C12** in H_2O (core only; open diamonds); **10_*d*C12** in D_2O (polymer and peptides only; open inverted triangles). Lines are best fit to a rod form factor. Error bars are shown.

H_2O) and the h- or d-hydrocarbon chains (see Table S1). Hence, there is likely to be a small contribution to the scattering from the peptidyl chains as well as the dodecyl hydrophobes.

Scattering data (with fits to the approriate rod model) are shown in Figure 4b, and the fit parameters are reported in Table 1. The peak at high Q is clearly evident in the shell contrast plot. The fitted core radius, R, obtained (20 Å) from the D/H/H contrast, is consistent with an extended C_{12} hydrocarbon chain (the calculated all-trans length of a C_{12} alkyl chain is 16.7 Å[27]) attached to peptidyl linkers, which add some radial length. These dimensions are clearly consistent with the independent fit obtained for the H/H/D contrast $R = 30$ Å, giving an estimate of 10 Å for the shell thickness. Hence, for the D/H/D sample data, the fit could be essentially calculated from the two solid rod fits giving R_{core} fixed as 20 Å, and the outer shell thickness, δ, to 10 Å, rod length, $L = 150$ Å. These parameters gave a good fit to the data, with only the scale factor required to vary to account for the change in ($\Delta\rho$; eq 1). Allowing a minor adjustment to the outer core radius refined the fit, giving $R_{total} = 34$ Å, within an entirely reasonable ±2 Å error of the calculated fit. The validity of the model over the three contrast sets increases confidence in the suitability of a rod-morphology and provides clear evidence for the elongated structure of these conjugates in solution and a core-shell structure of internalized hydrophobes.

Discussion

The similarity in scattering observed for conjugates **5_Ap** and **10_Ap** (i.e., with different loadings of aminopropanol terminated chains) is consistent with previous observations[20] and suggests that the degree of side-chain loading alone has little effect on conjugate conformation, except for a slight

Table 1. Conjugates Studied and Best-Fit Parameters Obtained from the SANS Analysis

conjugate details			SANS data fit parameters						
					rod model		core/shell rod model		
conjugate	mol % modification	substituent	Debye coil R_g/Å	R_g/Å calculated from rod parameters	L/Å	R/Å	L/Å	R_{core}/Å	δ/Å
5_Ap	2.5	aminopropanol	58						
10_Ap	8	aminopropanol	45						
5_ONp	2.5	*ortho*-nitrophenol	74						
10_ONp	8	*ortho*-nitrophenol		100	334	35			
5_*h*C12	2.5	*h*-dodecane		104	350	32			
10_*h*C12	8	*h*-dodecane		41	122	29			
10_*d*C12	8	*d*-dodecane		43			130	20	10

reduction in size at increased loading ($R_g = 55$ Å for **5_Ap** and 43 Å for **10_Ap**). An upturn in scattering at low Q is surprisingly more pronounced for the conjugate with the lower loading (5 mol % aminopropanol terminated side-chains, **5_Ap**). This suggests that the coil is slightly more open at the lower degree of side-chain loading, which introduces some weak intermolecular association (as seen by Ulbrich et al.[16]), whereas at the higher degree of loading intramolecular association drives a collapse of the coil, reflected in the lower R_g for this sample.

In keeping with previous observations for the clinical systems,[20,21] an upturn is not present in conjugates with larger side-chain terminating groups (*ortho*-nitrophenol or *h*-dodecyl), demonstrating that conjugation of the hydrophobic moiety disrupts intermolecular interactions between peptide chains.[20] This interruption occurs regardless of the aromatic/aliphatic nature of the conjugated molecules, however, it is evident that conjugates with different types of chain termination are affected differently by changes in side-chain loading.

For those conjugates that adopt a rod-like conformation (**10_ONp**, **5_*h*C12**, **10_*h*C12**, Figure 5), eq 2 enables the conversion of the fitted rod length (L) and cross-sectional radius (b) into an effective radius of gyration for the rod-like conjugates. This analysis provides a parameter through which to compare conjugates of all morphologies. Calculated R_g values (±5 Å) are given in Table 1.

$$R_g^2 = \frac{L^2}{12} + \frac{b^2}{2} \tag{2}$$

Modifying the peptide chains with either the aromatic or aliphatic molecules results in an increase in the observed R_g of the conjugate (compared to the aminopropanol capped equivalents), consistent with substitution causing an extension of the polymer backbone from the coiled (aminopropanol) state.

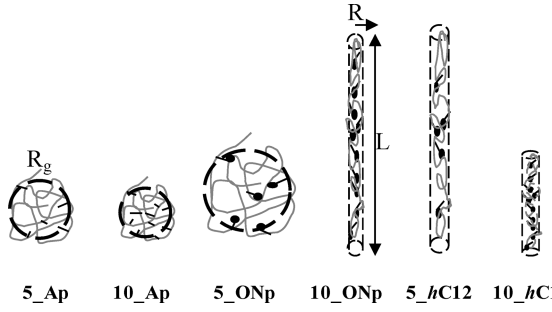

Figure 5. Schematic representation of the best-fit morphologies concluded from the SANS analysis. Representations are presented on a relative scale (solid gray line denotes polymer and linkers and solid black shapes represent hydrophobes).

For the aminopropanol terminated conjugates there is a decrease in R_g on increasing the side-chain loading. The same occurs for the *h*-dodecyl terminated conjugates, suggesting an increased interaction between the peptide chains and/or hydrophobes at the higher loading. At 5% modification, R_g for the *h*-dodecyl substituted conjugate (104 Å) is approximately twice that of the aminopropanol conjugate (58 Å), while at 10% modification R_g values for the two conjugates are very similar (41 and 45 Å, respectively). This is again supportive of an increased interaction between the side-chains at the higher degree of loading, which is enhanced by the presence of linear hydrophobes in the *h*-dodecyl substituted conjugate. Indeed, for the *h*-dodecyl conjugate, the contraction in fitted rod-length in conjunction with the consistency in radius between the 5% and 10 mol % dodecyl-modified samples leads us to propose the hypothesis of a helical-type conformation of the conjugate. The contraction in rod length could thereby be attributed to enhanced hydrophobic interactions between the linkers, an effect that is magnified by the presence of hydrophobes, increased lateral interactions along the length of which presumably stabilize the core of the structure and maintain the observed radius.

The *ortho*-nitrophenol containing conjugate is used here as a comparison of simple hydrophobic interactions versus $\pi-\pi$ interactions that are likely in the presence of an aromatic moiety. At 5% loading the **5_ONp** conjugate has a significantly larger R_g than the aminopropanol containing conjugate (**5_Ap**) conjugate, but still fits well to a random coil, indicating that at 5 mol % loading there is insufficient interaction between *ortho*-nitrophenol groups to cause significant perturbation of the polymer coil. In contrast, at 10 mol % the *ortho*-nitrophenol conjugate no longer fits to a coil model, indicative of enhanced interactions between the aromatic rings dominating the conformation.

Comparing fitted (**5_ONp**) and calculated (**10_ONp**) R_g values for the *ortho*-nitrophenol conjugates indicates a significant increase in R_g at the higher degree of loading. This increase in size with increased loading is in contrast to the decreases observed for aminopropanol and *h*-dodecyl-substituted systems but is keeping with observations for conjugates containing the aromatic drug Doxorubicin,[20] and more extensive studies are underway to determine the influence of increased aromatic conjugation on conjugate behavior.[28]

At the higher degree of loading the aromatic substituted (**10_ONp**) sample has a much larger R_g than the aliphatic (**10_*h*C12**) conjugate, by a factor of approximately 2.5. The rod-fit parameters also indicate a longer rod-length and slightly larger radius for the *ortho*-nitrophenol conjugate. Given the relative volumes of C_{12} and C_6(aromatic) groups (approximately 382 and 165 Å^3 molecule^{-1}, respectively[29]), the larger size of the *ortho*-nitrophenol conjugates here may be due to a reduced compatibility between the linkers and the aromatic drug mimic

samples, compared to the aliphatic dodecyl conjugates for which there may be more lateral interaction of the hydrophobic alkyl groups and the hydrophobic peptides. Reverting to our hypothesis of a helical arrangement, essentially to maintain $\pi-\pi$ stacking of the *ortho*-nitrophenol groups, the coils of the polymer may be pushed slightly further apart, resulting in an increased radius and longer rod length. This picture is also consistent with the contraction in size (rod length) observed with increased loading of simple linear hydrocarbon hydrophobes, whereby a closer overlap of the linear hydrophobes/peptidyl chains along the extended chain length pulls the rod/helix into a more densely packed (and therefore shorter) conformation.

The current data and analysis thereof represents a significant step forward in elucidating the detailed solution structure of these important and complex materials. It is clear that understanding solution conformation makes a significant input toward a better understanding of polymer−drug conjugate behavior overall, and these findings are likely to be of considerable benefit in the development of future conjugate systems, designed with favorable solution morphology in mind.

Conclusions

HPMA-*co*-MA-GFLG polymers with 5 or 10 mol % (feedstock ratios) peptidyl side chains capped with a simple aromatic *ortho*-nitrophenol group (ONp) have been modified by substitution of either an amino propanol (Ap) or linear dodecyl hydrocarbon chain (C_{12}). SANS experiments have shown there to be an influence of both the degree of modification and the type of hydrophobe present on the observed solution conformation. The added value of contrast-variation small-angle neutron scattering experiments has also been clearly demonstrated, and this methodology offers a unique insight into the microstructure of the conjugates in solution, allowing hydrophobe and polymer domains to be independently characterized. Data modeling for hydrophobically modified conjugates (C_{12} chain) has indicated a rod-like morphology of the scattering body, and contrast variation studies with deuterated hydrophobes provide clear evidence for a hydrophobe core surrounded by an outer polymer layer. For *ortho*-nitrophenol substituted groups a switch from random coil (also found for conjugates with no hydrophobic substituent added) to rod-like morphology was observed on increased *ortho*-nitrophenol loading. From conjugate structure dependent changes in rod-length and radius, we propose possible helical-type arrangement in solution, with the conformation ultimately dependent on the relative hydrophobic/$\pi-\pi$ interactions between the hydrophobes and the peptidyl linkers. Reviewing previous biological studies in the light of the recent data, it is clear that SANS experiments have a key role to play in elucidating links between biological activity and solution conformation.

Acknowledgment. STFC and ILL are thanked for the award of SANS beamtime and consumables funding. A.P. and C.J. acknowledge financial support from EPSRC and the School of Chemistry, Cardiff University for Ph.D. studentship and consumables funding (C.J.). Dr. M.-J. Vicent, Centro de Investigación Príncipe Felipe, Spain, is thanked for useful discussions regarding conjugate synthesis.

Supporting Information Available. Details of the conjugate synthesis, additional pairwise presentations of the raw scattering data, further information on the modeling process, including relevant equations, and a tabulated summary of the fitted parameters. This material is available free of charge via the Internet at http://pubs.acs.org.

References and Notes

(1) Duncan, R. *Nat. Rev. Drug Discovery* **2003**, *2* (5), 347–360.
(2) Duncan, R. *Biochem. Soc. Trans.* **2007**, *35*, 56–60.
(3) Duncan, R., Ringsdorf, H., Satchi-Fainaro, R., Eds. In *Polymer Therapeutics I: Polymers as Drugs, Conjugates and Gene Delivery Systems*; Springer: New York, 2006; Vol. 192, pp 1−8.
(4) Grayson, S. M.; Godbey, W. T. *J. Drug Target.* **2008**, *16*, 329–356.
(5) Han, H. D.; Lee, A.; Hwang, T.; Song, C. K.; Seong, H.; Hyun, J.; Shin, B. C. *J. Controlled Release* **2007**, *120*, 161–168.
(6) Kakizawa, Y.; Kataoka, K. *Adv. Drug Delivery Rev.* **2002**, *54*, 203–222.
(7) Putnam, D.; Kopecek, J. *Biopolymers II* **1995**, *122*, 55–123.
(8) Schmaljohann, D. *Adv. Drug Delivery Rev.* **2006**, *58*, 1655–1670.
(9) Abraham, A.; Nair, M. G.; Kisliuk, R. L.; Gaumont, Y.; Galivan, J. *J. Med. Chem.* **1990**, *33*, 711–717.
(10) Bruckdorfer, T. *Eur. Biopharm. Rev.* **2008**, 96, 98, 100, 102, 104.
(11) Hoes, C. J. T.; Grootoonk, J.; Duncan, R.; Hume, I. C.; Bhakoo, M.; Bouma, J. M. W.; Feijen, J. *J. Controlled Release* **1993**, *23*, 37–54.
(12) Maeda, H. *Adv. Drug Delivery Rev.* **1991**, *6*, 181–202.
(13) Ulbrich, K.; Subr, V.; Strohalm, J.; Plocova, D.; Jelinkova, M.; Rihova, B. In *Polymeric drugs based on conjugates of synthetic and natural macromolecules I. Synthesis and physico-chemical characterisation*, Proceedings of the 5th Symposium on Controlled Drug Delivery, Noordwijk Aan Zee, Netherlands, Apr 01−03, 1998, University of Twente, Enschede, The Netherlands, 1998; pp 63−79.
(14) Greco, F.; Vicent, M. J. *Frontier Biosci.* **2008**, *13*, 2744–2756.
(15) Kopecek, J.; Rejmanova, P.; Chytry, V. *Makromol. Chem.* **1981**, *182*, 799–809.
(16) Ulbrich, K.; Konak, C.; Tuzar, Z.; Kopecek, J. *Makromol. Chem.* **1987**, *188*, 1261–1272.
(17) Shiah, J. G.; Konak, C.; Spikes, J. D.; Kopecek, J. *J. Phys. Chem. B* **1997**, *101*, 6803–6809.
(18) Mendichi, R.; Rizzo, V.; Gigli, M.; Schieroni, A. G. *J. Appl. Polym. Sci.* **1998**, *70*, 329–338.
(19) Ding, H.; Kopeckova, P.; Kopecek, J. *J. Drug Targeting* **2007**, *15*, 465–474.
(20) Paul, A.; Vicent, M. J.; Duncan, R. *Biomacromolecules* **2007**, *8*, 1573–1579.
(21) Vicent, M. J.; Greco, F.; Nicholson, R. I.; Paul, A.; Griffiths, P. C.; Duncan, R. *Angew. Chem., Int. Ed.* **2005**, *44*, 4061–4066.
(22) Duncan, R.; Seymour, L. W.; O'Hare, K. B. *J. Controlled Release* **1991**, *19*, 331–346.
(23) Vasey, P. A.; Kaye, S. B.; Morrison, R.; Twelves, C.; Wilson, P.; Duncan, R.; Thomson, A. H.; Murray, L. S.; Hilditch, T. E.; Murray, T.; Burtles, S.; Fraier, D.; Frigerio, E.; Cassidy, J. *Clin. Cancer Res.* **1999**, *5*, 83–94.
(24) Polymer Laboratories Ltd., U.K., private communication.
(25) Heenan, R. K. *FISH*; Rutherford Appleton Laboratory: Didcot, U.K.
(26) Kojima, M.; Tanokura, M.; Maeda, M.; Kimura, K.; Amemiya, Y.; Kihara, H.; Takaha, K. *Biochemistry* **2000**, *39*, 1364–1372.
(27) Griffiths, P. C.; Paul, A.; Khayat, Z.; Heenan, R. K.; Ranganathan, R.; Grillo, I. *Soft Matter* **2005**, *1*, 152–149.
(28) Paul, A.; James, C. *Experimental report*; Institut Laue-Langevin, Grenoble, France, 2010.
(29) *ACD/ChemSketch Freeware*, version 10.00; Advanced Chemistry Development, Inc.: Toronto, ON, Canada, 2006; www.acdlabs.com.

BM1003338